INTERNATIONAL JOURNAL OF CLIMATOLOGY
Int. J. Climatol. **34**: 3702–3719 (2014)
Published online 14 February 2014 in Wiley Online Library
(wileyonlinelibrary.com) DOI: 10.1002/joc.3937

RMetS
Royal Meteorological Society

Spatial distribution of air temperature on Svalbard during 1 year with campaign measurements

R. Przybylak,[a]* A. Araźny,[a] Ø. Nordli,[b] R. Finkelnburg,[c] M. Kejna,[a] T. Budzik,[d] K. Migała,[e] S. Sikora,[e] D. Puczko,[f] K. Rymer[g] and G. Rachlewicz[g]

[a] *Department of Meteorology and Climatology, Nicolaus Copernicus University, Toruń, Poland*
[b] *Research and Development Department, Division for Model and Climate Analysis, Norwegian Meteorological Institute (MET Norway), Oslo, Norway*
[c] *Department of Ecology, Technical University, Berlin, Germany*
[d] *Department of Meteorology and Climatology, University of Silesia, Sosnowiec, Poland*
[e] *Department of Climatology and Atmospheric Protection, University of Wrocław, Poland*
[f] *Institute of Biochemistry and Biophysics PAS, Polish Academy of Sciences, Warsaw, Poland*
[g] *Cryosphere Research Department, Adam Mickiewicz University, Poznań, Poland*

ABSTRACT: In this article, the results of an investigation into the air temperature conditions on Svalbard in the period 1 September 2010 to 31 August 2011 are presented. For this period, parallel temperature measurements have been made as many as in 30 sites. On the basis of this unique set of data it was possible to study, in detail, the spatial distribution of different thermal characteristics [mean temperature, diurnal temperature range (DTR), day-to-day variability, degree of climate continentality, etc.] in Svalbard. Such knowledge of the whole of Svalbard was not previously available with sufficient accuracy for all areas. High resolution maps showing the spatial distribution of all studied thermal characteristics were also produced and analysed.

Analysis of surface temperature data shows that the markedly coldest area throughout the whole year was northern Svalbard, and in particular its eastern side (Nordaustlandet). On the other hand, the highest temperatures were recorded in western part of Spitsbergen. The greatest spatial decreasing rate of temperature in Svalbard throughout the whole year was observed in a southwest (SW)–northeast (NE) direction. The distribution of mean seasonal and annual temperature reduced to sea level on Svalbard differs from the distribution based on surface temperatures. Spring, and in particular winter, saw the greatest DTRs (4–7 and 6–9 °C, respectively), while the lowest were observed in summer (3.0–3.5 °C). In all seasons, the highest DTR were mainly noted in the NE part of Svalbard, while the lowest were in its SW part. The lowest continentality of climate (30%) is clearly seen in the south-western part of Svalbard, while the highest values (above 43%) stretch from the western part of Nordaustlandet to the area of Sveagruva in the central-eastern part of Spitsbergen. The NORA10 hindcast temperature data differ significantly from measured data for some seasons and areas and need bias corrections when used in climatology.

KEY WORDS Svalbard; Arctic; air temperature; historical climatology; climate change

Received 6 June 2013; Revised 2 January 2014; Accepted 3 January 2014

1. Introduction

Svalbard is an archipelago located in the warmest part of the Arctic. For example, the air temperature in winter is here about 20 °C higher than in the north-eastern part of the Canadian Arctic lying at the same latitude (Przybylak, 2003). The reason for this thermal privilege is the opening of the region to influences from the North Atlantic, expressed in the advection of warm and humid air and warm waters (including the significant influence of the West Spitsbergen Current (e.g. Walczowski and Piechura, 2011). As a result of this relatively easy access, Svalbard has quite often been the destination for many expeditions, both exploratory and scientific (e.g. Nathorst, 1909; Dybwad, 1913; Birkeland, 1920; Hoel, 1929; Szupryczyński, 2007 and references herein). Also one of the first meteorological stations in the Arctic located outside Greenland was established here in 1911 (Green Harbour). The climate history for Svalbard for almost the whole 20th century is quite well known (for details, see Steffensen, 1969; Steffensen, 1982; Hanssen-Bauer *et al.*, 1990; Steffensen *et al.*, 1996; Førland *et al.*, 1997; Przybylak, 2002; Przybylak, 2003; Przybylak, 2007; Nordli, 2010; Nordli *et al.*, 2014). On the other hand, markedly less is known about climate changes prior to this time. For the Holocen (including the last millennium), some information is available based on different proxy data (e.g. ice-cores and laminated lake sediments). For a short synthesis of this knowledge, see Przybylak (2003). Early-instrumental meteorological

* Correspondence to: R. Przybylak, Department of Meteorology and Climatology, Nicolaus Copernicus University, Toruń, Poland. E-mail: rp11@umk.pl

observations are available for some areas and time periods, but to compare them with the present-day climate, corrections are needed for the effect of different geographical locations of historical sites. But until now, knowledge about the spatial diversity of different thermal parameters for Svalbard has been limited due to the fact that almost all present meteorological stations are located only on the western coast of Spitsbergen. On the other hand, in the early instrumental period quite a lot of meteorological measurements have been made in the eastern and northern parts of the Svalbard archipelago. Therefore, to calculate climate change between historical and present times we need to know the spatial distribution of mean monthly and seasonal air temperatures throughout Svalbard with greater precision and reliability than has been possible until now. A review of the literature presenting the spatial distribution of temperatures on Svalbard confirms this statement (Dove, 1852; Hann, 1887; Birkeland, 1920; Alissow, 1954; Sochrina *et al.*, 1959; Treshnikov, 1985; Kotlyakov, 1998; Førland *et al.*, 2009). To improve existing knowledge about temperature differences on Svalbard, campaign measurements were performed with automatic weather stations (AWS) as part of the *Arctic Climate and Environment of the Nordic Seas and the Svalbard – Greenland Area* (AWAKE) project. The AWS were located at historical sites in Svalbard, where old meteorological stations had previously been operating as well as in the Forlandsundet region, as part of climatological studies conducted by the Department of Meteorology and Climatology of the Nicolaus Copernicus University since 1975 (Przybylak *et al.*, 2012). In addition, all other available temperature data from Svalbard have been used. These come from currently running synoptic weather stations, as well as from sites located in Hornsund and Petunia (near Pyramiden) regions, where investigations by Polish universities and institutions have been performed, and finally from the Nordaustlandet island, in an investigation conducted within the IPY-KINNVIKA project (Change and variability of Arctic systems Nordaustlandet, Svalbard). On the basis of the parallel measurements conducted from 1 September 2010 to 31 August 2011 at all these sites, for the first time, the density of stations was sufficient to describe spatial distribution of temperature on the entire Svalbard archipelago. The main aim of this article is to present the synthesis of these investigations and to make available to climate studies new maps with distributions of some of the temperature parameters on Svalbard.

2. Area, data and methods

Svalbard is an archipelago belonging to the Norwegian Arctic located between latitudes 74°–81° north, and longitudes 10°–35° east. Spitsbergen is the largest island, followed by Nordaustlandet and Edgeøya (Figure 1).

The location of all sites on Svalbard where temperature measurements have been made in the period 1 September 2010 to 31 August 2011 is shown in Figure 1, while the names of sites (including acronyms) and their geographical coordinates are given in Table 1. Altogether, data from 30 sites have been gathered for analysis. As can be seen, the majority are mainly located in the western part of Svalbard, however, some also lie in northern and eastern parts of the area.

Meteorological data used in this article comes from different institutions [Norwegian Meteorological Institute (MET Norway), the Arctic and Antarctic Research Institute in St. Petersburg, the Institute of Geophysics and Polish Academy of Sciences in Warsaw] and from four Polish universities (the Nicolaus Copernicus University in Toruń, the University of Wrocław, the University of Silesia in Sosnowiec and the Adam Mickiewicz University in Poznań) and one German university (the Technical University in Berlin). Temperature measurements on Svalbard were conducted using AWS (Vaisala, Campbell), temperature sensors (DIN TC Ltd. Pt-100 1/10, MadgeTech and HOBO) located 2 m above ground, as well as radiation screens, usually of the MI-2001 and Onset RSI types (for details see Table A1 of Appendix). Different accuracy of temperature sensors (0.1–0.6 °C) used for measurements can influence the results, if the errors are not stochastic. Parallel temperature measurements in the Forlandsundet region carried out in tundra and glacial environments, using both the temperature sensors and mercury thermometers with the respective accuracy of 0.5 and 0.1 °C (both thermometers were placed in Stevenson screens) have shown either a lack or very small and not statistically significant differences between the calculated daily and monthly means. This means that the different accuracy of temperature sensors did not influence the results presented in the article. Quality control of the data was conducted by the owners or suppliers of the data. A small number of gaps were filled using data from nearby stations. For the analysis, daily mean temperatures as well as daily maximum and minimum temperatures have been taken as source data.

Diurnal temperature range (DTR) was calculated according to definition, by subtracting daily minimum temperature (Tmin) from daily maximum temperature (Tmax). To calculate day-to-day (interdiurnal) temperature variability (DDTV) series of differences were established between consecutive days of daily mean temperatures. The chosen measure for DDTV was standard deviation (SD) applied to the series of differences within each month, as well as for each season. Annual temperature range (ATR) was calculated by subtracting the mean temperature of the coldest month from the mean temperature of the warmest month.

To estimate the continentality/oceanicity of the climate in Svalbard, indices proposed by Ewert (1972) and Marsz (1995) have been used. The continentality index proposed by Ewert was calculated according to the formula:

$$K = \left[\mathrm{ATR} - \frac{(3.81 \cdot \sin\phi + 0.1)}{(38.39 \cdot \sin\phi + 7.47)}\right] 100\%$$

where ATR is annual temperature range, and φ is the geographical latitude.

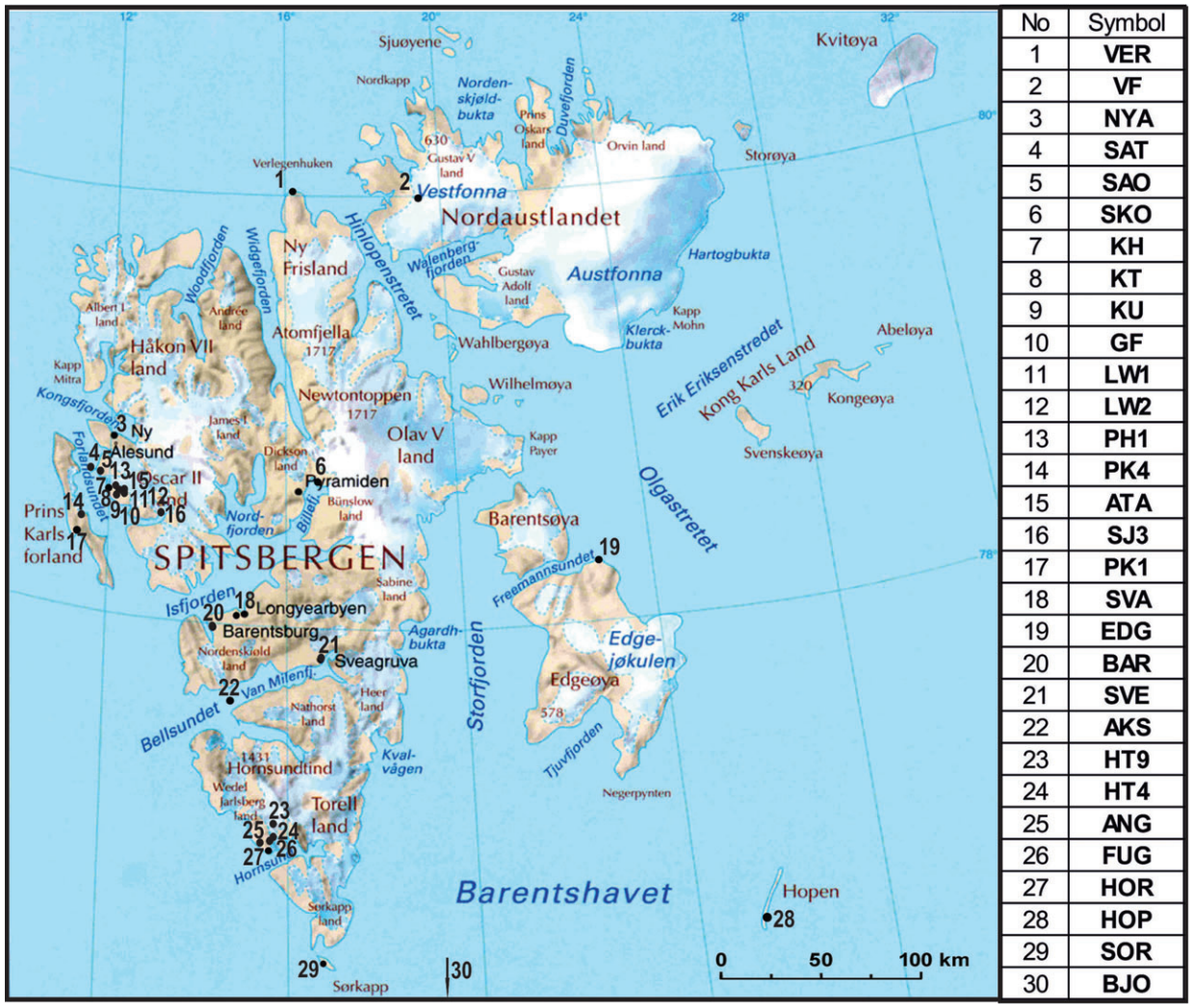

No	Symbol
1	VER
2	VF
3	NYA
4	SAT
5	SAO
6	SKO
7	KH
8	KT
9	KU
10	GF
11	LW1
12	LW2
13	PH1
14	PK4
15	ATA
16	SJ3
17	PK1
18	SVA
19	EDG
20	BAR
21	SVE
22	AKS
23	HT9
24	HT4
25	ANG
26	FUG
27	HOR
28	HOP
29	SOR
30	BJO

Figure 1. Location of meteorological sites in Svalbard from which data were used (for explanation of acronyms see Table 1).

This index takes into account the dependence of ATR not only on geographical latitude, but also on the percentage of land in a given latitudinal band, relief, condensation processes, etc. Index K changes around the world from 0% for areas with extreme oceanic climate to more than 140% for the extremely continental part of Eastern Siberia (Ewert, 1997). This index can be calculated for each place on the Earth without any exception (Okołowicz, 1976). For the entire Arctic, the index was calculated by Ewert (1997) and his map, presenting the spatial distribution of the index, is also available in Przybylak (2003). In their recent work, Hogewind and Bissolli (2011) calculated the continentality index using a modification of the Ivanov's (1959) formula for the WMO Region VI, which includes the Norwegian Arctic.

Marsz (1995) stated that because oceans dominate the earth, one can speak about the decreasing influence of oceans with increased distance from their coasts. Therefore he proposed use of an index of oceanicity of climate (Oc):$\mathrm{Oc} = \frac{(0.732\phi + 1.767)}{\mathrm{ATR}}$

On the basis of the distribution of values of this index around the world, Marsz (1995) distinguished the following types of climate: ultracontinental ($\mathrm{Oc} < 1$), continental (Oc from 1.00 to 1.99), suboceanic (Oc from 2.00 to 2.99), oceanic (Oc from 3.00 to 3.99) and ultraoceanic ($\mathrm{Oc} > 3.99$).

In order to eliminate the influence of altitude on mean monthly, seasonal and annual air temperature, a reduction to sea level was made using a lapse rate of 0.6 °C per 100 m. Division of the year into seasons was made following a proposition given by Putnins *et al.* (1959) and Gavrilova and Sokolov (1969). For winter, they include the months from November to March, for spring April and May, for summer June, July and August, and for autumn September and October.

As seen from Figure 1, the temperature network (Table 2) is distributed unevenly, being mostly located on the western coastal part of Svalbard and concentrated mainly in two regions. Therefore, for the maps presented in this article, data from 14 stations, roughly evenly distributed in the Svalbard area, have been used (VER, VF, NYA, SKO, KH, PK1, SVA, EDG, BAR, SVE, AKS, HOR, HOP and SOR). For drawing of isotherms, one of the most frequent methods of interpolation has been

Table 1. Location of meteorological sites in Svalbard from which data were used.

Number	Symbol	Site	Φ	λ	*h* (m a.s.l.)
1	VER	Verlegenhuken	80°04′N	16°15′E	8
2	VF	Vestfonna	79°59′N	19°28′E	370
3	NYA	Ny-Ålesund	78°55′N	11°56′E	8
4	SAT	Sarstangen	78°44′N	11°29′E	2
5	SAO	Sarsøyra	78°43′N	11°43′E	9
6	SKO	Skotehytta	78°42′N	16°37′E	5
7	KH	Kaffiøyra-Heggodden	78°41′N	11°50′E	11
8	KT	Terasa	78°41′N	11°58′E	90
9	KU	Kuven	78°41′N	12°01′E	193
10	GF	Gråfjellet	78°41′N	12°01′E	345
11	LW1	Waldemar Glacier-Front	78°41′N	12°00′E	130
12	LW2	Waldemar Glacier-Firn field	78°41′N	12°05′E	375
13	PH1	Prins Heinrichfjella-1	78°41′N	11°59′E	500
14	PK4	Prins Karls Forland-East	78°41′N	11°59′E	6
15	ATA	ATA-Hus	78°40′N	11°59′E	137
16	SJ3	St. Jonsfjord-Muton	78°34′N	13°09′E	14
17	PK1	Prins Karls Forland-West	78°28′N	11°12′E	9
18	SVA	Svalbard Lufthavn	78°15′N	15°28′E	28
19	EDG	Edgeøya-Kapp Heuglin	78°15′N	22°49′E	14
20	BAR	Barentsburg	78°04′N	14°15′E	70
21	SVE	Sveagruva	77°53′N	16°43′E	9
22	AKS	Akseløya	77°41′N	14°47′E	6
23	HT9	Hansbreen-Firn field	77°11′N	15°48′E	421
24	HT4	Hansbreen-Middle	77°04′N	15°63′E	184
25	ANG	Angelfjellet	77°04′N	15°15′E	380
26	FUG	Fugleberget	77°00′N	15°34′E	568
27	HOR	Hornsund	77°00′N	15°33′E	10
28	HOP	Hopen	76°31′N	25°01′E	6
29	SOR	Sørkappøya	76°29′N	16°33′E	10
30	BJO	Bjørnøya	74°31′N	19°00′E	16

Data from stations marked by grey shading have been used to draw Figures 3–7

used, i.e. point kriging, using a linear variogram model (Ustrnul and Czekierda, 2003). For more details see also Isaaks and Srivastava (1989).

As compensation for the lack of an accurate observational dataset with high spatial resolution, a regional high-resolution (∼11 km) hindcast archive (Reistad *et al.*, 2011; Haakenstad *et al.*, 2012) has been developed at MET Norway. The archive is called NORA10 and covers the period from September 1957 until present. It contains hourly fields of surface- and near-surface parameters, and fields in the 40 model levels (wind, temperature and humidity) every third hour.

NORA10 is produced by dynamical downscaling, running a frozen version of the HIRLAM NWP model (version 6.4.2, Undén *et al.*, 2002) for an area covering the north-eastern North Atlantic, including Scandinavia. Forcing data have been ERA40 (Uppala *et al.*, 2005) for the period September 1957 to August 2002, and operational European Centre for Medium-Range Weather Forecasts (ECMWF) analyses from September 2002 to present. The operational ECMWF analyses have at the moment a horizontal resolution of 16 km.

3. Results and discussion

One year of observations is the minimum time period for studying mean temperature differences on Svalbard for all months and seasons, and throughout the whole year. Of course, longer periods are preferable, but maintaining AWS in remote areas with difficult access by sea, such as the northern and eastern parts of Svalbard, is very difficult and expensive. When the AWAKE and KINNVIKA projects were concluded, the AWS had to be removed from the most distant areas.

Before beginning an analysis of temperature distribution on Svalbard in the study period, a description of the conditions of atmospheric circulation, sea surface temperature (SST) and sea ice can be useful. The features of atmospheric circulation on Svalbard in the period of July 2010 to August 2011 were studied by Przybylak and Maszewski (2012a), as well as the influence of atmospheric circulation on air temperature in the Forlandsundet region (Przybylak and Maszewski, 2012b). Generally, when the entire period of observation is taken into account there were no significant differences between the study period and the long-term period of 1950–2006. Anomalies in the relative frequency of occurrence of nine distinguished synoptic types generally do not exceed 4% (see Figure 2.3 in Przybylak and Maszewski, 2012a). However, a clearly greater frequency than normal reveals cyclonic situations, while anticyclonic situations were more rare. Particularly extreme atmospheric circulation occurred in March, April and October when positive anomalies of cyclonic situations varied from 28.9% in

Table 2. Mean monthly, seasonal and annual air temperatures (°C) in Svalbard in the period from September 2010 to August 2011.

Site	Sep	Oct	Nov	Dec	Jan	Feb	Mar	Apr	May	Jun	Jul	Aug	Autumn	Winter	Spring	Summer	Sep to Aug
VER	*0.0*	−3.6	−12.7	−14.7	−16.9	−12.8	−16.4	−8.8	−4.4	0.3	3.5	3.6	*−1.8*	−14.7	−6.6	2.5	*−6.9*
VF	−3.2	−7.3	−18.5	−20.0	−22.3	−16.4	−19.8	−11.6	−7.3	−0.3	1.1	0.7	−5.2	−19.4	−9.5	0.5	−10.4
NYA	1.2	−3.4	−11.6	−10.9	−13.9	−10.7	−12.7	−5.3	−2.0	3.8	6.3	5.7	−1.1	−12.0	−3.7	5.3	−4.5
SAT	2.3	−1.5	−8.6	−8.8	−13.7	−11.3	−9.8	−3.8	−1.1	4.1	6.0	5.5	0.4	−10.4	−2.5	5.2	−3.4
SAO	1.8	−2.8	−10.6	−10.2	−13.6	−10.1	−11.1	−4.8	−1.6	3.9	6.3	6.0	−0.5	−11.1	−3.2	5.4	−3.9
SKO	1.9	−2.9	−13.0	−13.1	−15.9	−16.2	−14.5	−6.6	*−2.0*	*5.0*	*7.1*	*7.0*	−0.5	−14.5	*−4.3*	*6.4*	*−5.3*
KH	1.9	−2.2	−9.4	−9.2	−13.6	−10.5	−10.5	−4.2	−1.4	4.0	5.9	5.5	−0.2	−10.6	−2.8	5.1	−3.6
KT	2.0	−2.3	−9.9	−9.3	−12.5	−8.4	−10.0	−3.7	−1.2	4.3	6.4	6.5	−0.2	−10.0	−2.5	5.7	−3.2
KU	1.4	−3.0	−10.4	−9.8	−12.6	−8.6	−10.7	−4.5	−2.3	3.3	5.4	5.8	−0.8	−10.4	−3.4	4.8	−3.8
GF	0.8	−3.9	−11.1	−10.6	−13.0	−9.4	−12.0	−5.7	−3.7	2.0	4.3	5.2	−1.6	−11.2	−4.7	3.8	−4.8
LW1	1.6	−2.9	−10.4	−9.7	−12.7	−8.7	−10.5	−4.1	−1.1	3.7	5.4	6.0	−0.7	−10.4	−2.6	5.0	−3.6
LW2	0.8	−4.1	−11.6	−10.9	−13.3	−9.3	−11.8	−5.1	−2.2	3.3	4.2	4.5	−1.7	−11.4	−3.7	4.0	−4.6
PH1	0.3	−5.3	−12.5	−12.1	−13.9	−10.5	−13.1	−5.9	−2.6	3.8	4.5	4.7	−2.5	−12.4	−4.3	4.3	−5.2
PK4	2.3	−1.8	−9.2	−8.9	−12.9	−9.5	−10.1	−4.2	−1.4	3.7	6.4	6.3	0.3	−10.1	−2.8	5.5	−3.3
ATA	1.6	−2.9	−10.8	−9.9	−13.2	−8.9	−10.5	−4.2	−1.2	4.2	6.2	6.1	−0.7	−10.7	−2.7	5.5	−3.6
SJ3	2.2	−2.4	−10.4	−10.3	−13.3	−9.5	−11.3	−4.4	−1.4	3.5	5.6	5.7	−0.1	−11.0	−2.9	4.9	−3.8
PK1	2.4	−2.0	−9.5	−9.2	−12.4	−9.0	−10.4	−4.2	−1.4	3.9	6.4	6.5	0.2	−10.1	−2.8	5.6	−3.2
SVA	2.0	−2.9	−11.0	−11.6	−15.2	−12.7	−12.7	−5.8	−1.6	4.8	6.9	6.9	−0.5	−12.7	−3.7	6.2	−4.4
EDG	*1.7*	−2.0	−12.4	−15.4	−19.1	−15.6	−14.3	−8.7	−4.2	0.0	2.1	2.4	*−0.1*	−15.4	−6.5	1.5	*−7.1*
BAR	1.3	−3.1	−10.3	−10.8	−14.5	−12.1	−12.2	−5.7	−2.0	4.1	6.6	6.2	−0.9	−12.0	−3.9	5.6	−4.4
SVE	1.7	−3.5	−13.3	−15.2	−17.4	−14.0	−14.9	−7.2	−2.7	3.8	6.0	5.5	−0.9	−15.0	−5.0	5.1	−5.9
AKS	2.0	−1.6	−8.3	−11.3	−16.1	−12.2	−13.0	−5.8	−2.4	2.9	4.4	4.9	0.2	−12.2	−4.1	4.0	−4.7
HT9	−0.5	*−5.5*	*−12.5*	−13.5	−15.9	−12.2	−12.9	−6.7	−4.5	0.8	2.1	2.1	*−3.0*	*−13.4*	−5.6	1.6	*−6.6*
HT4	1.3	−3.9	−10.8	−11.4	−13.9	−10.4	−11.7	−4.7	−2.9	1.6	2.6	2.9	−1.3	−11.6	−3.8	2.4	−5.1
ANG	0.4	−4.1	−10.8	−11.2	−13.4	−10.0	−11.3	−5.4	−3.7	1.5	3.5	4.7	−1.8	−11.4	−4.6	3.2	−5.0
FUG	−0.8	−5.2	−12.1	−12.7	*−15.1*	*−11.7*	−13.0	−7.0	−5.1	0.1	2.1	3.0	−3.0	*−12.9*	−6.1	1.7	*−6.5*
HOR	2.5	−2.0	−8.4	−9.5	−12.5	−9.4	−9.8	−3.7	−1.6	3.2	3.9	4.2	0.3	−9.9	−2.7	3.8	−3.6
HOP	2.2	−0.1	−7.0	−10.1	−14.2	−11.2	−10.4	−4.3	−3.0	0.0	2.4	3.2	1.0	−10.6	−3.6	1.9	−4.4
SOR	*2.2*	*−0.4*	*−7.4*	−10.8	−14.0	−11.7	−9.1	−4.8	−2.2	1.0	2.0	3.2	*0.9*	*−10.6*	−3.5	2.1	*−4.3*
BJO	4.0	1.2	−3.6	−4.1	−6.5	−4.1	−4.7	0.7	0.3	1.9	4.7	5.9	2.6	−4.6	0.5	4.2	−0.4

Seasons: autumn (September to October), winter (November to March), spring (April to May), summer (June to August); data marked by grey shading have been used to draw Figures 3–7; statistically approximated values are shown using italic font.

October to 34.6% in April. On the other hand, the frequency of anticyclonic situations was largely below normal (from −25.9% in October to −38.9% in April). For example, April which was the most anomalous month, was characterized by significantly less advection of air masses from northern and eastern sectors for anticyclonic situations (by about 15–16%), and for cyclonic situations there was also a significant excess of airflow from southern and eastern sectors (by about 17 and 11%, respectively) (for more details see Table 2.4 in Przybylak and Maszewski 2012a).

Warm Atlantic waters coming with the West Spitsbergen Current are particularly important, due to the latter's great influence on the Svalbard climate. In recent years, the temperature and salinity of the Atlantic waters have significantly risen (Walczowski and Piechura 2011). The system of oceanic currents and the heat exchange between the ocean and the atmosphere influence the range and concentration of sea ice. The extent of Arctic sea ice during the modern satellite record period (1979 to present) shows a downward trend in all months, with the smallest in winter and the largest at the end of the summer melt season in September (Stroeve *et al.*, 2012). In the analysed period, the area of sea ice cover in the Arctic remained below the long-term average value. In 2010 in the area of Spitsbergen at the time of the most intense propagation of sea ice (April), the west coast was free of ice, while in the east it reached Sørkapp (the southern tip of Spitsbergen). In July that year, most of the ice melted and in October the sea ice moved away from the archipelago to the north. However, in January 2011 the sea ice reoccurred, covering the sea east of Spitsbergen and spreading to the northeast coast in April. In July the sea ice remained along the east coast and, floating with the oceanic currents, went around Sørkapp, blocked the entrance of the Isfjorden and reached Kaffiøyra. In spite of this, in September 2011 the extent of the sea ice in the Arctic had shrunk to a record low of 4.24 million km^2, or 0.6% less than in the previous record-breaking summer of 2007 (http://www.iup.uni-bremen.de:8084/amsr/minimum2011-en.pdf). Increased SST and the reduction of extent of sea ice also affected the air temperature and precipitation on Spitsbergen in the analysed period.

3.1. Surface air temperature

Although it is not the main purpose of this article, we want to first describe the results of temperature at real altitudes, based on data from 30 sites (Table 2) as well as from the NORA10 hindcast archive (see Chapter 2 in Reistad *et al.*, 2011) calculated for the same periods (Figure 2).

In order to establish a reference for the short study period in a longer time perspective, temperature was compared with mean normal values from 1971 to 2000, based on data from the long-term meteorological stations. The majority of months in the study period were warmer than in the last three decades of the 20th century. April was particularly warm, with mean temperatures exceeding the normal by more than 5 °C. Anomalous atmospheric circulation in that month, described earlier here and in more details by Przybylak and Maszewski (2012a), is mainly responsible for this temperature anomaly. Only November and January were colder than normal, but not in all areas (Table 3). In these 2 months, cold conditions can be explained by the markedly lower frequency of advection of air masses from the southern sector (see Table 2.4 in Przybylak and Maszewski, 2012a).

In all seasons, the clearly coldest conditions occurred in the northern part of Svalbard and in particular in its eastern part (Nordaustlandet; Table 2 and Figure 2). Some areas in eastern-central Spitsbergen are also quite cold, e.g. Skotehytta and Sveagruva. In general, the warmest temperatures were noted during winter in the western part of Spitsbergen, heated as it is by the West Spitsbergen Current, and by warm and moist air masses coming with cyclones moving from Iceland to Kara Sea. In summer, the central part of Spitsbergen is very warm (if not the warmest), which has a high degree of climate continentality and is covered relatively less by glaciers in comparison with other areas (Hisdal, 1985; Hagen *et al.*, 1993). Svalbard Airport had the highest temperature in all summer months, out of all stations, reaching the mean temperature for summer 6.2 °C (Table 2). On the other hand, in winter the lowest mean temperature falls below −20 °C in the inner, glaciated part of Nordaustlandet (Vestfonna and Austfonna) and also in mountain areas located in northern Spitsbergen (Figure 2). Spring was clearly colder than autumn by 1–3 °C. This can be explained by the fact that usually in spring, the frequency of anticyclones is greater than in autumn (see the statistics for circulation pattern 5, Figure 3 in Käsmacher and Schneider, 2011; Láska *et al.*, 2012), cloudiness is lower, and coverage by snow and sea ice is greater (Przybylak, 1992). In the study period, this was also the case (for details see Przybylak and Maszewski, 2012b and Kejna, 2012). Mean annual temperature varied from about −4 °C on western coastal parts of Spitsbergen to less than −12 °C in mountain and glaciated areas of northern Svalbard. Generally, the greatest decreasing rate of temperature in Svalbard throughout the whole year is observed in a southwest (SW)–northeast (NE) direction.

3.2. Temperature at sea level

The majority of the meteorological observations carried out in the Svalbard archipelago in historical times were limited to the coastal parts, thus the altitude of temperature measurements was near sea level. In the eastern and northern parts of Svalbard there are no regular meteorological stations, but for historical times (the 19th century and the beginning of 20th century) quite a lot of short measurement series exist. Thus to reliably calculate temperature change between historical and present times for these areas, temperatures for the contemporary period are needed. For this purpose, data taken from permanent stations currently working only in the western part

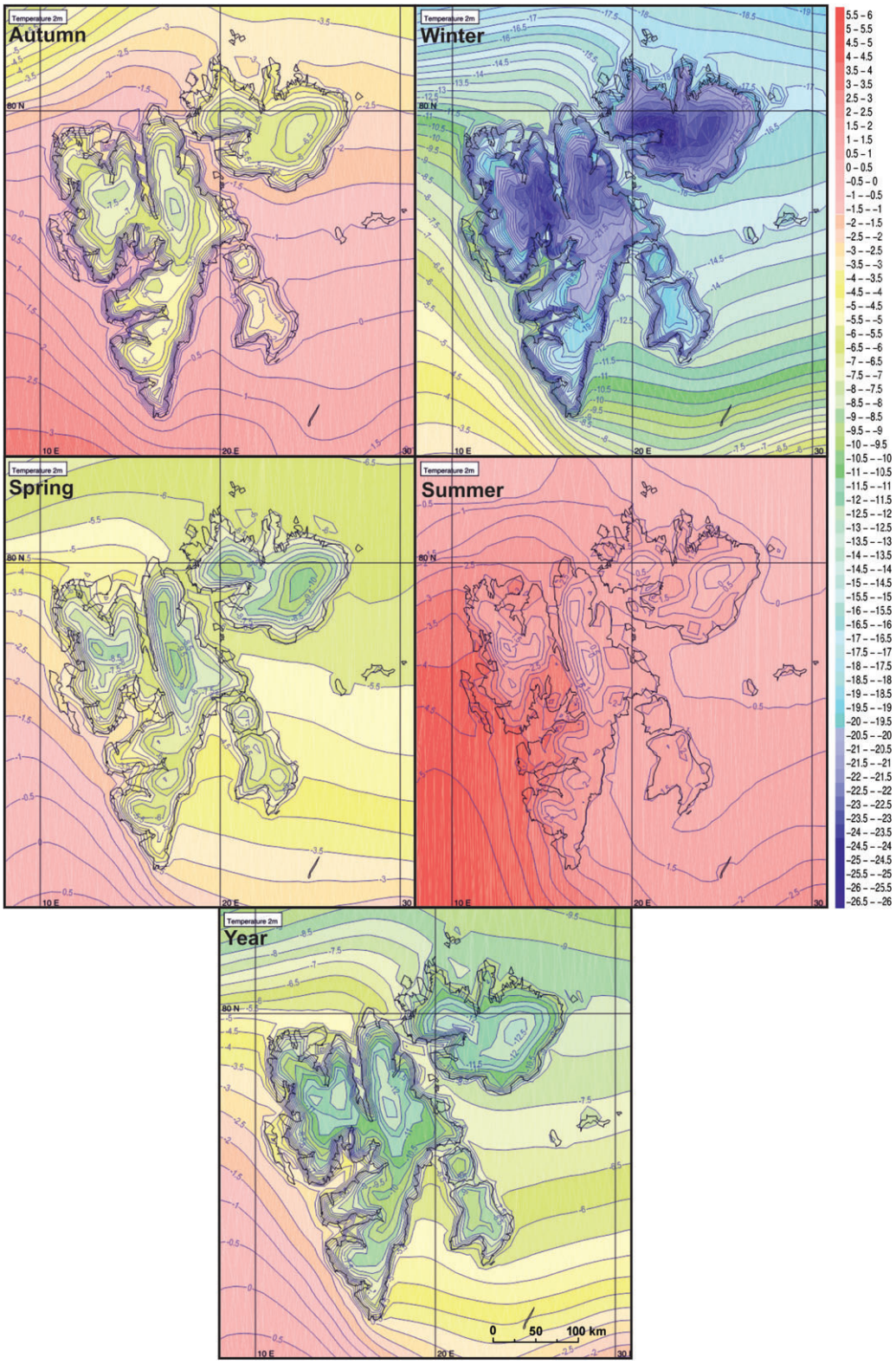

Figure 2. Mean surface seasonal and annual air temperature (°C) in Svalbard using the NORA10 model fields September 2010 to August 2011.

of Svalbard can be used. But we need also information about the spatial diversity of temperatures on Svalbard and that is why the main aim of this article is to supply such knowledge. To obtain more reliable data, the influence of different altitudes of measurement sites on temperature has to be eliminated. Therefore, all gathered air temperature data were reduced to sea level using a lapse rate of 0.6 °C per 100 m. On the basis of such sets of data constructed for 14 stations (Table 1), isotherms can be drawn with the required resolution for both seasons (Figure 3) and months (Figures A1 and A2 of Appendix). Having such maps, the mean long-term temperature can

Table 3. Monthly mean anomalies of air temperature (°C) in Svalbard (period September 2010 to August 2011 in relation to reference period 1971–2000; Araźny, 2008).

Site	Sep	Oct	Nov	Dec	Jan	Feb	Mar	Apr	May	Jun	Jul	Aug
NYA	1.2	2.2	−3.1	1.2	−0.4	3.6	0.1	5.1	1.5	2.1	1.4	1.7
SVA	1.3	2.4	−2.0	1.0	−0.5	2.7	0.9	5.5	2.1	2.5	0.7	1.9
HOR	1.2	1.6	−1.3	1.4	−0.6	2.3	0.6	5.5	1.6	1.5	−0.4	0.3
HOP	1.0	2.9	0.8	1.4	−1.5	1.5	1.1	6.2	1.4	0.1	0.1	0.3
BJO	1.0	1.5	−0.2	2.2	0.4	2.7	1.3	5.6	1.4	−0.2	0.0	1.0

be calculated for each point of Svalbard, and compared with data for the same point in historical time. As a result, the influence of different geographical locations (in historical and present times) of temperature measurement sites can be eliminated. If the reader requires greater resolution of isotherms, we have also included source data for monthly means (Table 2) for all 30 stations, which can be used for this purpose.

Spatial distribution of mean seasonal and annual temperature reduced to sea level differ from that based on surface temperatures, but a general decrease of temperature from SW to NE is seen in both cases, except in summer and autumn. In summer, the temperature at sea level is highest in the central part of Spitsbergen (about 6 °C) and decreases to the north, east and south. However, the lowest values (about 2 °C) are noted in the outer eastern part of Svalbard (Figure 3). In autumn, latitudinal distribution of temperature across the whole of Svalbard is observed. The highest temperature (about 0.5 °C) occurred in the southern part of Svalbard, while the lowest (−1.5 to −2.5 °C) in the northern part, and in particular in its eastern part. The temperature range in Svalbard was highest in winter (November to March), varying from about −10 °C in the SW part of Spitsbergen to −17 °C in the northern part of Nordaustlandet island. On Spitsbergen the isotherms run longitudinal in this season (the effect of strong cyclonic activity in this time of the year), while to the east of Spitsbergen they run latitudinal, which is also the effect of cyclonic activity having a stronger influence on southern than northern parts of the area, as well as of differences in sea ice coverage (more open water in the south). In spring, the pattern of temperature changes is similar as in winter, but decreasing rate from SW to NE is smaller. In the study period the temperature varied from −3 to −7 °C, which was appreciably colder than in autumn.

All maps presented spatial distribution of temperature on Svalbard (Figure 3 and Figures A1 and A2) after elimination of the strong influence of altitude on temperature, can also be used to study the influence of other factors (e.g. latitude, sea currents and kinds of surface coverage) on temperature, but this analysis is outside the scope of the present work.

From this high quality set of daily temperature data for Svalbard for the period 1 September 2010 to 31 August 2011, for 14 sites, various other thermal characteristics [DDTV, DTR, ATR and certain indices of climate continentality (K) and oceanicity (Oc)] have also been calculated, and their spatial distributions are shown in Figures 4–6. In the case of DDTV, the patterns of spatial distribution in the four seasons are different. In winter, the temperature is most stable in the western part of Svalbard (DDTV slightly higher than 5 °C) and highest in its eastern-central part near the Sveagruva station (DDTV about 7 °C). Isolines mainly have a longitudinal run and the values of DDTV in this season are markedly higher than in other seasons (Figure 4). The most stable mean daily temperature is clearly in summer. Values of DDTV varied from 1 °C (in southern part) to about 2 °C in the central part of Spitsbergen. The northern part of the study region saw only a slightly smaller temperature variability in comparison to the central part. Surprisingly high DDTV occurred in spring, which is usually the season of highest frequency of occurrence of anticyclones in Svalbard and the Arctic as a whole (Przybylak, 2003; Käsmacher and Schneider, 2011). However, as mentioned earlier, this was not the case in spring 2011. Cyclones clearly dominated in this season, in particular in April (Przybylak and Maszewski, 2012a) and as a result of this anomaly an increase in DDTV was observed. Its values varied from about 3 °C in the SW to more than 5 °C on Nordaustlandet Island. Both patterns of spatial changes of DDTV in Svalbard as well as its values in autumn are most similar to those noted in summer (Figure 4). The greatest values of DDTV calculated for the whole year occurred in the NE part of Svalbard (more than 4.4 °C) with the maximum near Sveagruva station. On the other hand, the smallest values occurred in the south-western and western parts of Svalbard (less than 4 °C).

DTR on Svalbard is the lowest in the Arctic and according to Przybylak (2000) its annual values in the period 1951–1990 varied between 5 and 6 °C. Almost the same range of DTR was noted in the study period when its annual values varied from 4.5 °C (in the southern and western parts) to 6 °C in the northern and central-eastern parts of Spitsbergen (Figure 5). The highest DTR occurred in winter (caused by a vigorous and changeable cyclonic activity, Przybylak, 2003, p. 86); and in spring were only slightly smaller (relatively large daily contrast of solar radiation, for details see e.g. Ohmura, 1984). In both seasons the smallest DTR were observed in the western part of Svalbard (about 5.5–6.0 °C in winter and 4.5–5.0 °C in spring), while the highest were in the central-eastern part in winter (more than 8 °C), and the north-eastern part in spring (more than 7 °C). In both seasons the greatest spatial gradient of DTR

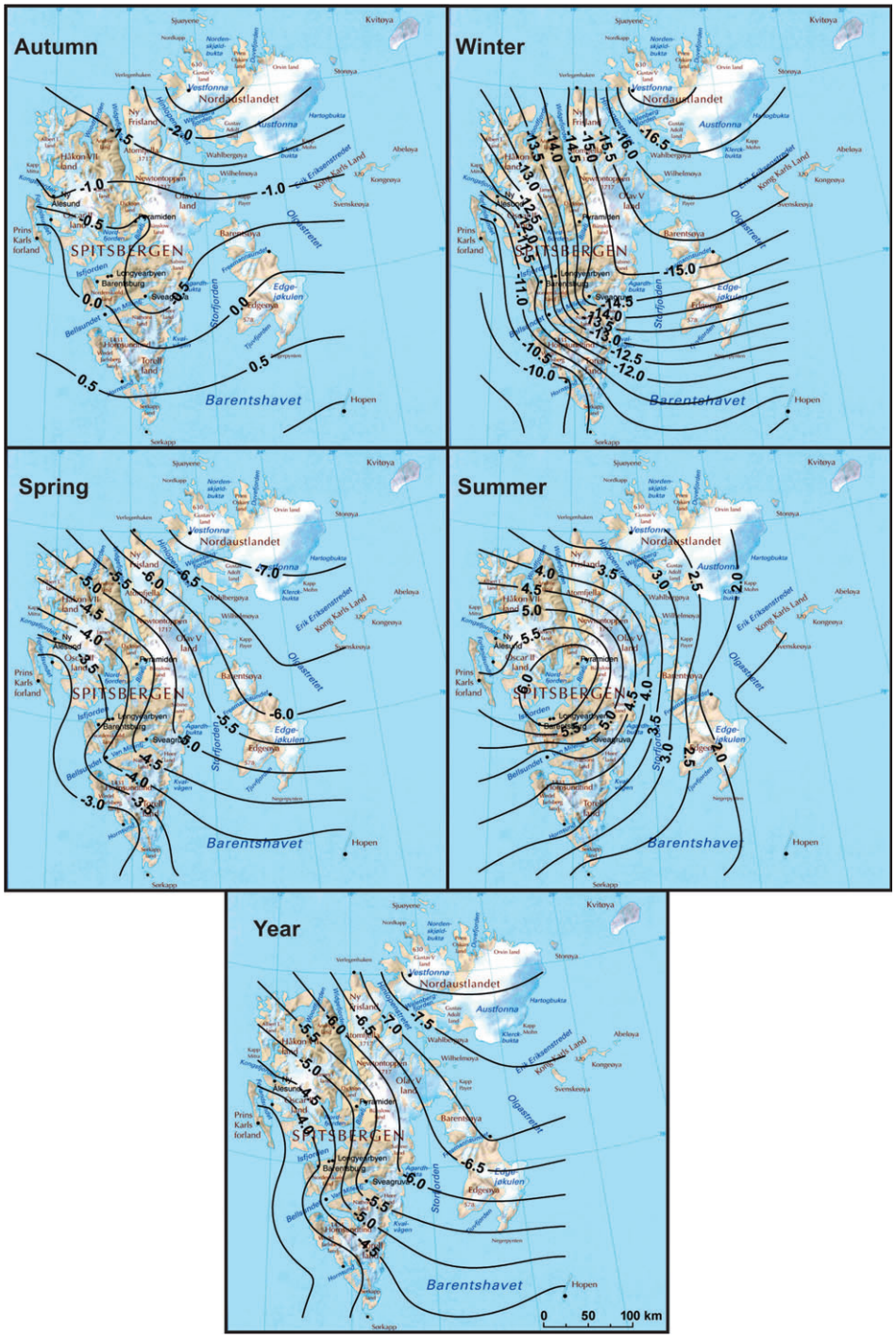

Figure 3. Mean seasonal and annual air temperature (°C) at sea level in Svalbard (September 2010 to August 2011).

was observed from west to east in the central part of Spitsbergen (Figure 5). On the other hand, spatial patterns of DTR and their values were very similar in autumn and summer. In summer the DTR was slightly higher than in autumn in the southern part of Svalbard (3.0–3.5 *vs* 3.0 °C), while the opposite relation is seen for the northern part (3.5 *vs* 4.0 °C). In summer, spatial differences of DTR are smaller by 0.5 °C than in autumn, and generally in summer the DTR is stable throughout the whole of Svalbard, excluding its most outer southern part (Figure 5).

One of the most synthetic measures of climate based on which it is possible to describe roughly the most important features of climate of a given area is the ATR, which is usually calculated as the temperature difference between warmest and coldest months. On Svalbard, as shown from Figure 6 (upper left map), the greatest values of ATR (above 23 °C) occurred in its north-eastern part, while the lowest in the southern, western and – in particular – the south-western parts of Svalbard (below 17 °C). In the southern part of Svalbard the isolines run latitudinal (increase of ATR to the north),

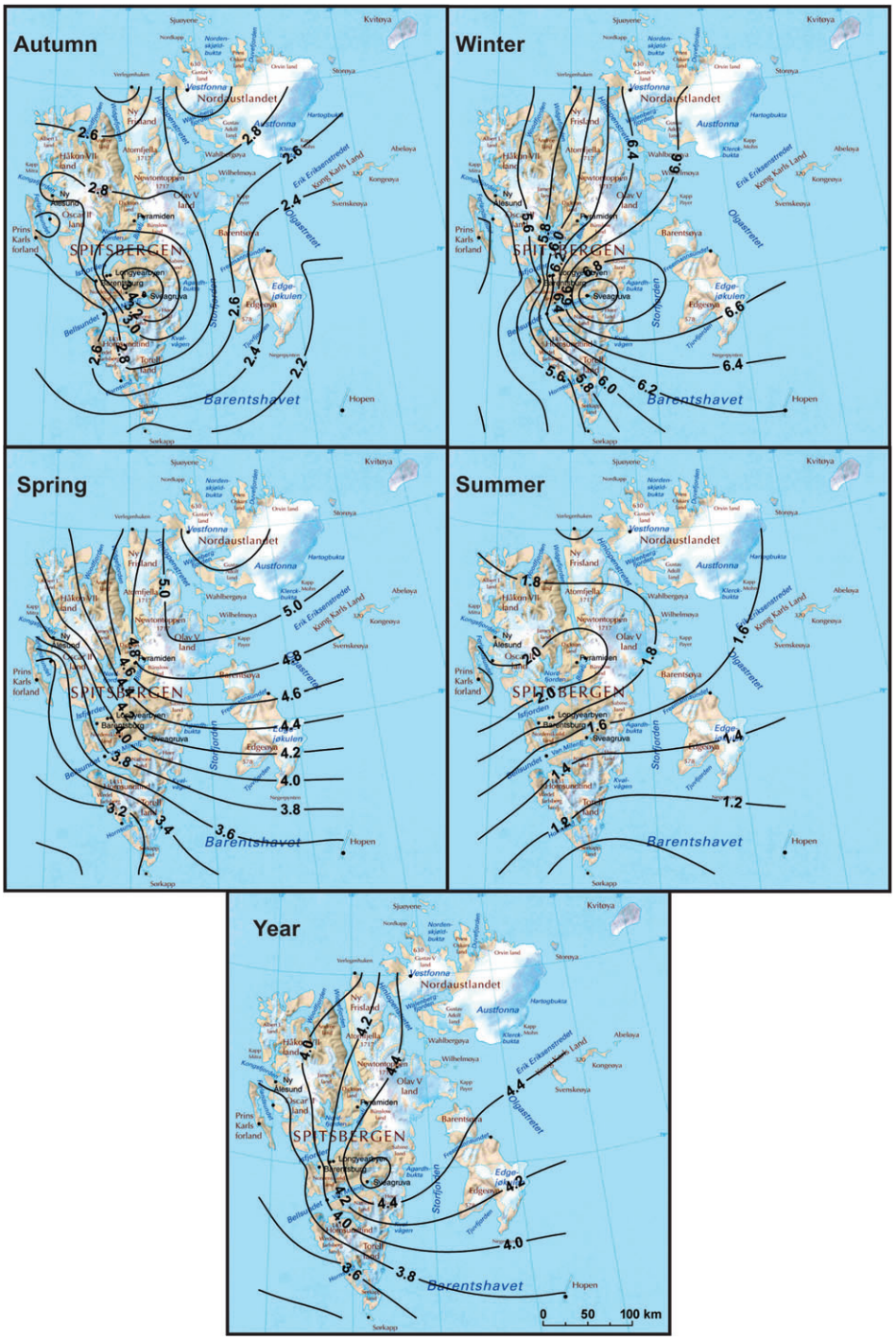

Figure 4. Seasonal and annual standard deviation of mean daily temperature (SD,°C) in Svalbard, September 2010 to August 2011.

while in the northern part they run longitudinal (increase of ATR to the east). ATR allows for rough estimation of the continentality of climate, but to be more precise in describing the continentality, latitude should also be taken into account. Indices of thermic continentality of climate and/or thermic oceanicity, which both take into account the influence of latitude on continentality, have been calculated to exactly investigate spatial differences of this climate feature in Svalbard (Figure 6). Analysis of maps presented in Figure 6, however, lead to the conclusion that in Svalbard's case the influence of geographical latitude on thermic continentality/oceanicity is very small. Evidence of this can be seen in the fact that patterns of spatial changes of climate continentality, expressed using three different measures (ATR, K and Oc), are very similar. Ewert (1997) calculated the thermic continentality of climate for the whole Arctic, including Svalbard, based on long-term data. For Svalbard, the continentality index varied from 30% (in the southern and western parts) to 40% (in the north-eastern part) with a resolution of 10%. In Figure 6 (upper right map), the thermic continentality of climate, according to

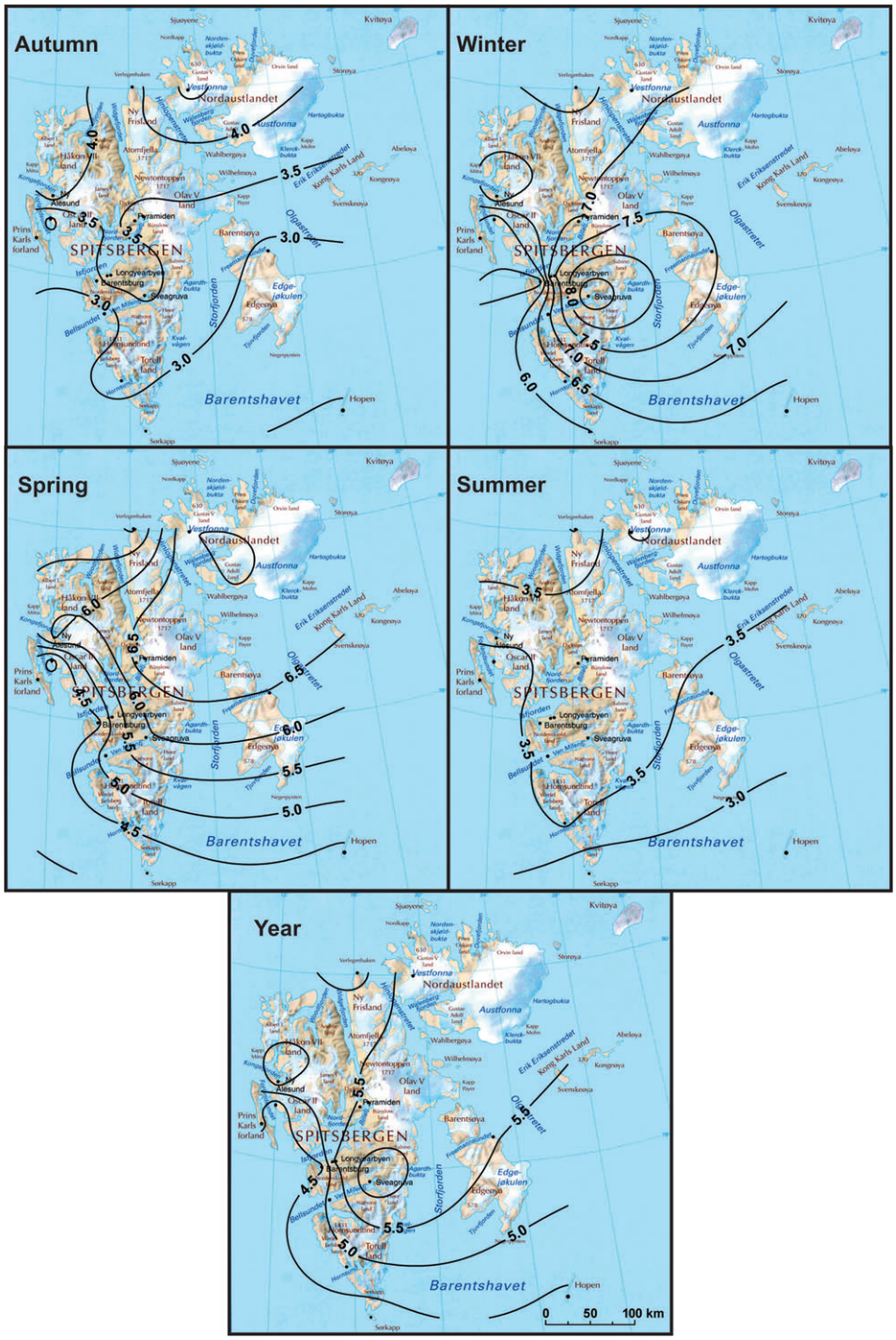

Figure 5. Mean seasonal and annual diurnal temperature range (DTR, °C) in Svalbard, September 2010 to August 2011.

Ewert's formula, is estimated with 1% resolution. This allows more detailed analysis of the spatial changes of thermic continentality of climate in Svalbard. Although the values of the index are almost the same in Ewert's map (from 30 to 40%) and in our map (30 to 43%), the run of isolines differ significantly. Lower continentality of climate (30%) is clearly seen in the south-western part of Svalbard (in Ewert's map, the western coast also has the same degree of continentality), while the highest values (above 43%) stretch out from the western part of Nordaustlandet to the area of Sveagruva in the central-east part of Spitsbergen (in Ewert's map, limited only to NW Nordaustlandet).

3.3. Hindcast *versus* instrumental data

The hindcast archive (NORA10) offers a tool for studying the Svalbard climate at 10–11 km resolution. The question is how far the results turn out to be in agreement with the measurements. Using the present, dense network, this was checked against seasonal and annual

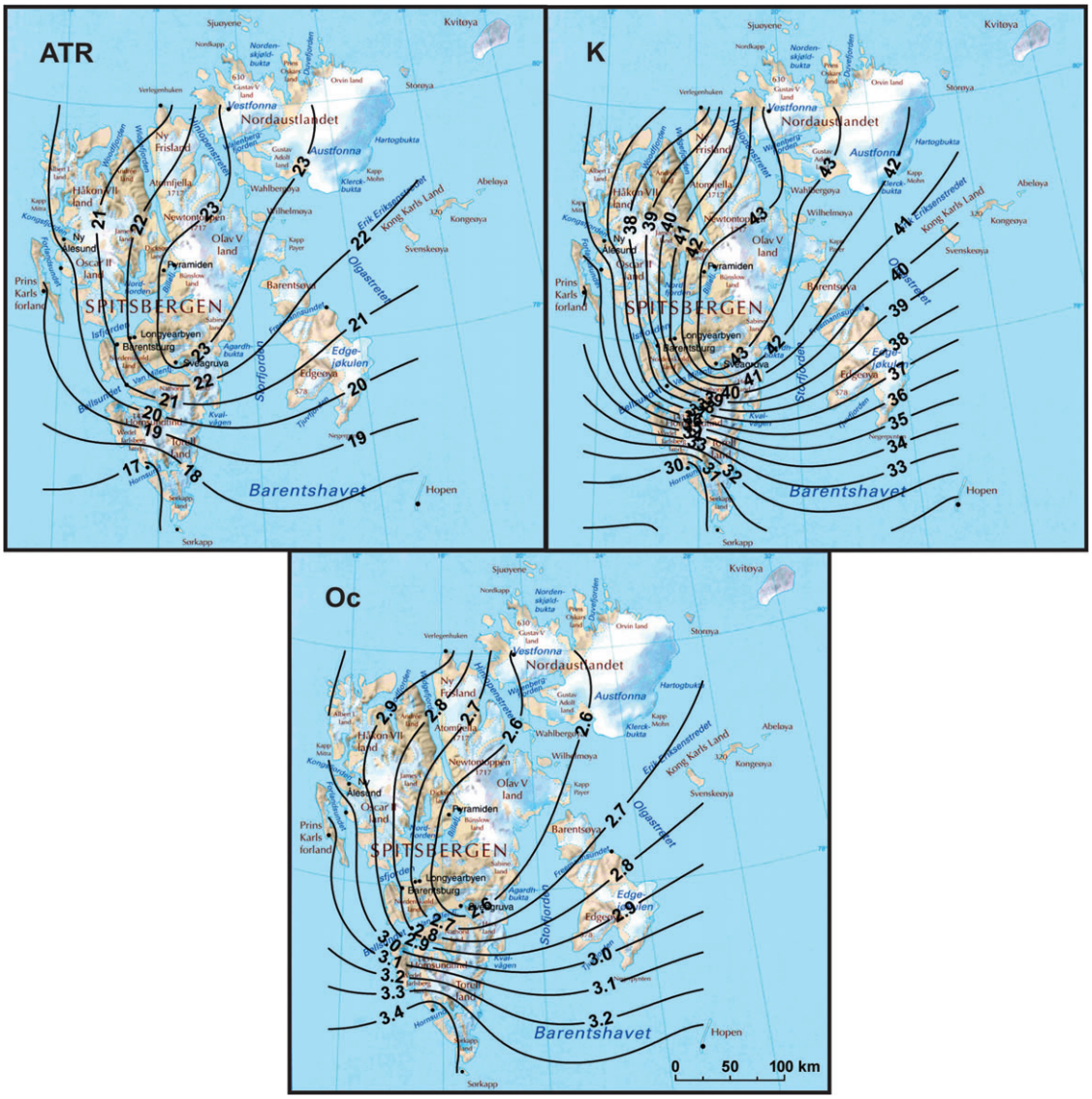

Figure 6. Annual range of air temperature (ATR, °C), thermal climate continentality index (K) according Ewert's (1972) formula and thermal oceanicity index (Oc), according to Marsz's (1995) formula, in Svalbard, September 2010 to August 2011.

mean temperatures based on observations. However, the NORA10 dataset consists of grid points that will usually not be located exactly at the sites of the meteorological stations, although the distance between a station and the nearest grid point has to be less than about 7 km. For topography like that of Svalbard's, there might, on some occasions, be appreciable differences in altitude. Therefore we have applied adjustments for height differences (by −0.6 °C per 100 m). The differences between the NORA10 data and instrumental data taken from the period 1 September 2010 to 31 August 2011 are shown in Figure 7. As can be seen, temperature differences differ between seasons, and within seasons there are also spatial variations. Modelled temperatures in the larger part of Svalbard are too cold in all seasons in the central part of Svalbard. Positive differences are mainly observed in northern, western and (to a lesser degree) in southern outer parts of Svalbard. In winter, differences between NORA10 and instrumental data reached their maximum value, varying −3 °C in the region near Pyramiden to 5 °C in the Bellsund area. Outside these two regions, the differences are usually less than 2 °C. According to Przybylak (2002), SD of winter temperature is here about 3 °C. This means that differences are smaller everywhere than 2 SD. In summer and spring, temperature differences seldom exceed 2 °C, varying mainly between −1 and 1 °C (Figure 7). However, because the summer temperature is four times more stable than the spring's (SD equal to about 0.5 and 2 °C, respectively), the NORA10 data are relatively more biassed for summer than for the other seasons, in particular for the area stretching from Pyramiden to Sveagruva and Longyearbyen (error greater than 4 SD). On the other hand, in the spring the temperature differences, except in the northern part, are less than 1 SD. Thus, in this season the fit to the observations are the best out of all seasons. Errors for annual values in the majority of the Svalbard area do not exceed 2 SD. Again, similar to all seasonal patterns, the central

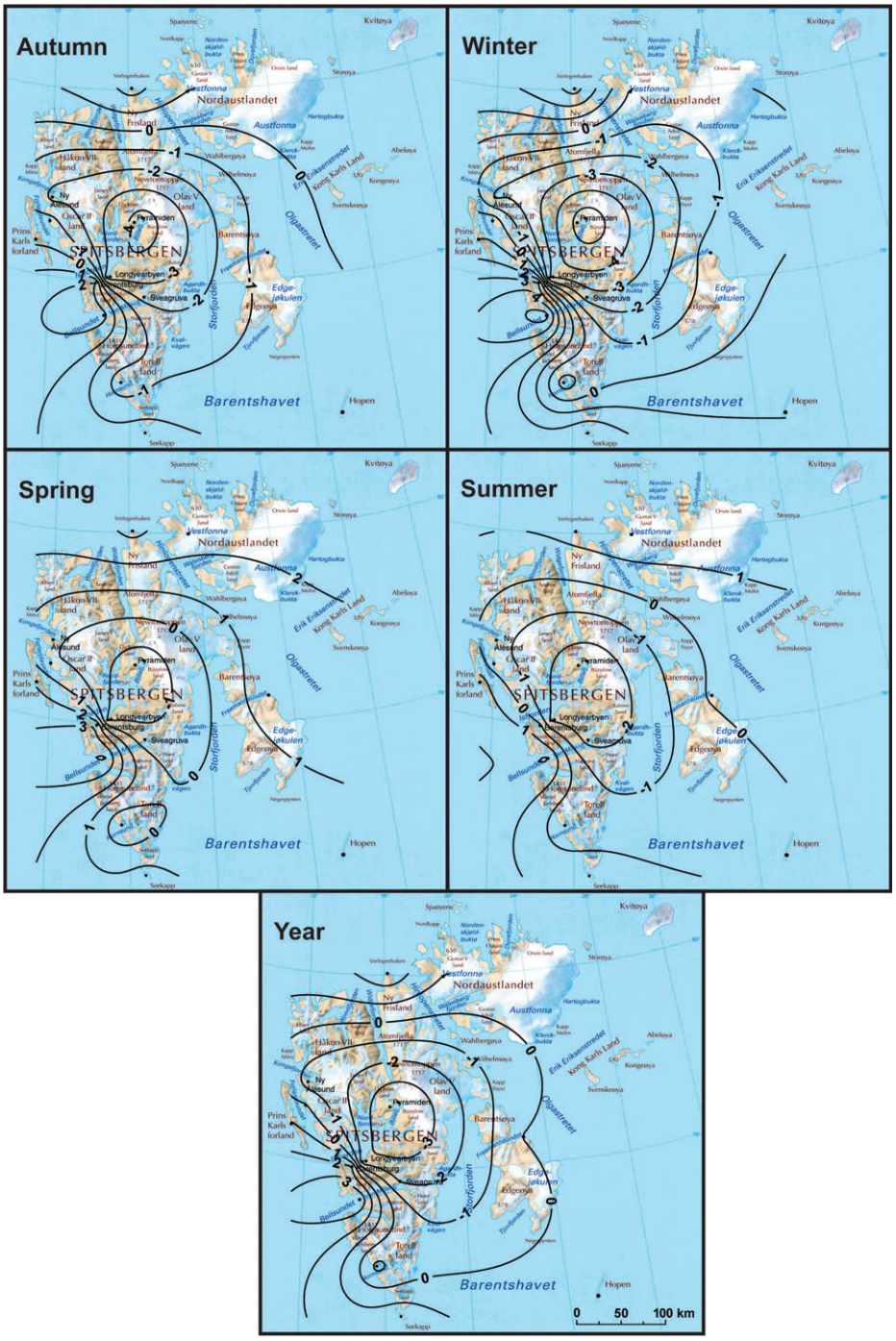

Figure 7. Mean seasonal and annual temperature differences (°C) between the hindcast data from the NORA10 and measured instrumental data on Svalbard, September 2010 to August 2011.

part of Spitsbergen shows the greatest differences, both positive and negative (3 and −3 °C, respectively). The model also differs appreciably over short distances, making bias corrections of model results difficult. Partly, this may be explained by local variations smaller than the model resolution of 10 km.

4. Final remarks and conclusions

From the Second World War to the 4th International Polar Year (2007–2009) there were no meteorological stations in the eastern and northern parts of Svalbard robust enough to stand against the Arctic environment, including the interest of polar bears. All regular meteorological stations as well as sites of meteorological measurements established by different national expeditions were located on the western coast. Surprisingly, quite a lot of meteorological measurements in the eastern and northern parts of Svalbard have been conducted historically, in particular around the end of the 19th century, i.e. at a time when regular meteorological observations in Svalbard had still not begun. The recent, intensified

measurement campaigns in the remote and uninhabited parts of Svalbard covering the period 1 September 2010 to 31 August 2011 (via the AWAKE and KINNVIKA projects), has significantly improved our knowledge of the spatial distribution of different meteorological elements, particularly including air temperature, which is a subject of analysis in this article. However, full climate analysis for this area needs a denser network of stations and longer periods of observations, which is impossible to do within scientific projects the duration of which is generally not longer than 3 years. The need for a regular meteorological station in this area is high. Hopefully, the improved robustness of the stations on Edgeøya, Kongsøya and Kvitøya will fulfil this need, as the data coverage so far (spring 2013) is promising, (*cf* http://eklima.met.no for a free download).

Summing up, it must be underlined that for the first time in the history of meteorological observations in Svalbard, parallel meteorological measurements for the whole area have only been made in the period 1 September 2010 to 31 August 2011. Use of these data can be manifold. For example, they could be used to study climate changes in eastern and northern parts of Svalbard between historical and present times. In this article we have used them to study the spatial distribution of different thermal characteristics in Svalbard and to check the quality of the hindcast NORA10 data set. Two of the stations, Akseløya and Sørkappøya, are AWS re-established on historical sites so that statistical relationships between data from these sites and Svalbard Airport could be developed. The relationships have already been used to prolong the Svalbard Airport temperature series back to 1898 (Nordli *et al.*, 2014).

The main results of this article can be summarized as follows:

1. Svalbard in the study period was significantly warmer than in the period 1971–2000. In particular, April saw mean warmth higher by more than 5 °C. Only November and January were colder than the normal, but not in all areas.
2. Throughout the whole year, the northern areas of Svalbard are the coldest, in particular its eastern part (Nordaustlandet). On the other hand, clearly warmer temperatures were noted in the western part of Spitsbergen, which is heated by the West Spitsbergen Current and by warm and moist air masses coming in with cyclones moving from Iceland to the Kara Sea. In summer, the central part of Spitsbergen is also very warm – if not the warmest – having a great degree of climate continentality and being covered by relatively less glaciation in comparison with other areas. The greatest spatially decreasing rate of temperature in Svalbard throughout the whole year is observed in a SW to NE direction.
3. Patterns of distribution of mean seasonal and annual temperature reduced to sea level on Svalbard differ from those based on real temperatures; however, a general decrease of temperature from SW to NE is seen in both cases, except summer and autumn.
4. In all seasons (except summer), the temperature reduced to sea level is the highest/lowest in the SW/NE parts of Svalbard. In summer the highest/lowest temperatures occur in the central-west and eastern parts of Svalbard, respectively.
5. The most stable temperature conditions from day-to-day occur in summer, in particular in the southern part of Svalbard (SD < 1 °C), while the greatest variability is observed in winter, particularly in the central-eastern part (SD > 7 °C).
6. Spring, and in particular winter, saw the greatest DTR (4–7 and 6–9 °C, respectively), while the lowest were observed in summer (3.0–3.5 °C). In all seasons the highest DTR were mainly noted in the NE part of Svalbard, and the lowest in its SW part.
7. The lowest continentality of climate (30%) is clearly seen in the south-western part of Svalbard, while the highest values (above 43%) stretch out from the western part of Nordaustlandet to the area of Sveagruva in the central-east part of Spitsbergen.
8. The NORA10 hindcast temperature data differ appreciably from the measured data for some seasons and areas. In particular, large errors exceeding 4 SD were found for summer temperatures limited, however, to the central part of Spitsbergen. In other seasons errors usually do not exceed values of 2 SD. The model fit differs greatly over the Svalbard area, and also with biases of different signs.

Acknowledgements

The research work of Andrzej Araźny, Marek Kejna and Rajmund Przybylak described in this article was supported by the Polish-Norwegian Fund as part of the Arctic Climate and Environment of the Nordic Seas and the Svalbard-Greenland Area project (AWAKE and AWAKE 2) and by the grant 'Contemporary and historical changes in the Svalbard climate and topoclimates' funded by the National Science Centre by decision No. DEC-2011/03/B/ST10/05007. We would like to express our gratitude to Matthias Braun, Marco Möller, Dieter Scherer and Christoph Schneider for their important contributions in the matters of Vestfonna data [Grant Nos BR 2105/6-1, SCHE 750/3-1, SCHE 750/3-2, SCHN 680/2-1, SCHN 680/2-2 of the German Research Foundation (DFG) and Grant Nos 03F0623A and 03F0623B of the German Federal Ministry of Education and Research (BMBF)]. Likewise we want to thank Ragnar Brækkan (MET Norway) for designing new, robust meteorological stations for Arctic conditions, a work of paramount importance. Hilde Haakenstad (MET Norway) should be particularly acknowledged for her work on the NORA10 data.

Appendix

See Table A1; Figures A1 and A2

Table A1. Information on meteorological sites, air temperature sensors and their radiation screens used on Svalbard in the period 1 September 2010 to 31 August 2011.

No	Site*	Kind of station	Name, producer and type of sensor	Accuracy of temperature sensor (°C)	Type of radiation screen	Ventilation (forced or passive)	Data gaps
1	Verlegenhuken	C	Pt-100, TC ltd., 1/10 DIN	±0.1	MI-2001	Passive	1 September to 30 September
2	Vestfonna	C	Campbell Sci., CS215	± 0.6	Thies 1.1025.55.100	Forced	–
3	Ny-Ålesund	P	Pt-100, TC ltd., 1/10 DIN	±0.1	MI-2001	Passive	–
4	Sarstangen	C	MadgeTech, Temp110	±0.5	Onset RS1	Passive	–
5	Sarsøyra	C	MadgeTech, Temp110	±0.5	Onset RS1	Passive	–
6	Skotehytta	C	HOBO, Onset	±0.5	Onset RS1	Passive	1 May to 31 August
7	Kaffiøyra-Heggodden	C	MadgeTech, Temp110	±0.5	Onset RS1	Passive	–
8	Terasa	C	MadgeTech, Temp110	±0.5	Onset RS1	Passive	–
9	Kuven	C	MadgeTech, Temp110	±0.5	Onset RS1	Passive	–
10	Gråfjellet	C	MadgeTech, Temp110	±0.5	Onset RS1	Passive	–
11	Waldemar Glacier-Front	C	MadgeTech, Temp110	±0.5	Onset RS1	Passive	–
12	Waldemar Glacier-Firn field	C	MadgeTech, Temp110	±0.5	Onset RS1	Passive	–
13	Prins Heinrichfjella-1	C	MadgeTech, Temp110	±0.5	Onset RS1	Passive	–
14	Prins Karls Forland-East	C	MadgeTech, Temp110	±0.5	Onset RS1	Passive	–
15	ATA-Hus	C	MadgeTech, Temp110	±0.5	Onset RS1	Passive	–
16	St. Jonsfjord-Muton	C	MadgeTech, Temp110	±0.5	Onset RS1	Passive	–
17	Prins Karls Forland-West	C	MadgeTech, Temp110	±0.5	Onset RS1	Passive	–
18	Svalbard Lufthavn	P	Pt-100, TC ltd., 1/10 DIN	±0.1	MI-2001	Passive	–
19	Edgeøya-Kapp Heuglin	C	Pt-100, TC ltd., 1/10 DIN	±0.1	MI-2001	Passive	1 August to30 September
20	Barentsburg	P	Mercury thermometer	±0.2	Instrument shelter	Passive	–
21	Sveagruva	P	Pt-100, TC ltd., 1/10 DIN	±0.1	MI-2001	Passive	–
22	Akseløya	C	Pt-100, TC ltd., 1/10 DIN	±0.1	MI-2001	Passive	–
23	Hansbreen-Firn field	C	Vaisala HMP45AC	±0.2	Campbell URS1 Gill	Passive	1 to 30 November
24	Hansbreen-Middle	C	Vaisala, HMP45AC	±0.2	Campbell URS1 Gill	Passive	–
25	Angelfjellet	C	HOBO U23, Onset	±0.2	Onset RS3	Passive	–
26	Fugleberget	C	HOBO U23, Onset	±0.2	Onset RS3	Passive	1 January to 4 March
27	Hornsund	P	Vaisala , HMP45D	±0.2	Vaisala, DTR13	Passive	–
28	Hopen	P	Pt-100, TC ltd., 1/10 DIN	±0.1	MI-2001	Passive	–
29	Sørkappøya	C	Pt-100, TC ltd., 1/10 DIN	±0.1	MI-2001	Passive	1 September to 30 November
30	Bjørnøya	P	Pt-100, TC ltd., 1/10 DIN	±0.1	MI-2001	Passive	–

C, campaign; P, permanent.
*Resolution data at all stations 1 hour, the check data quality.

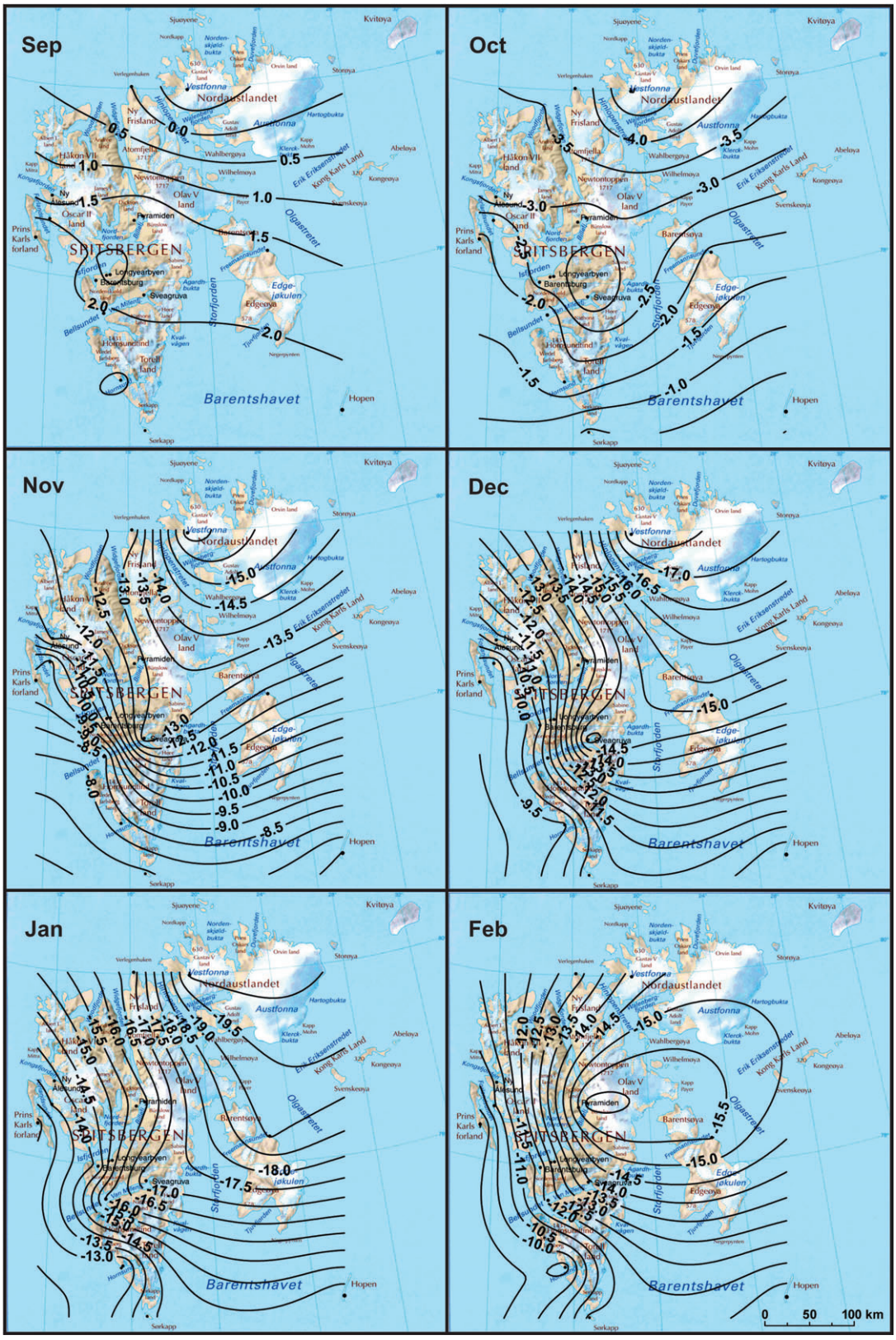

Figure A1. Mean monthly air temperature (°C) at sea level in Svalbard (September 2010 to February 2011).

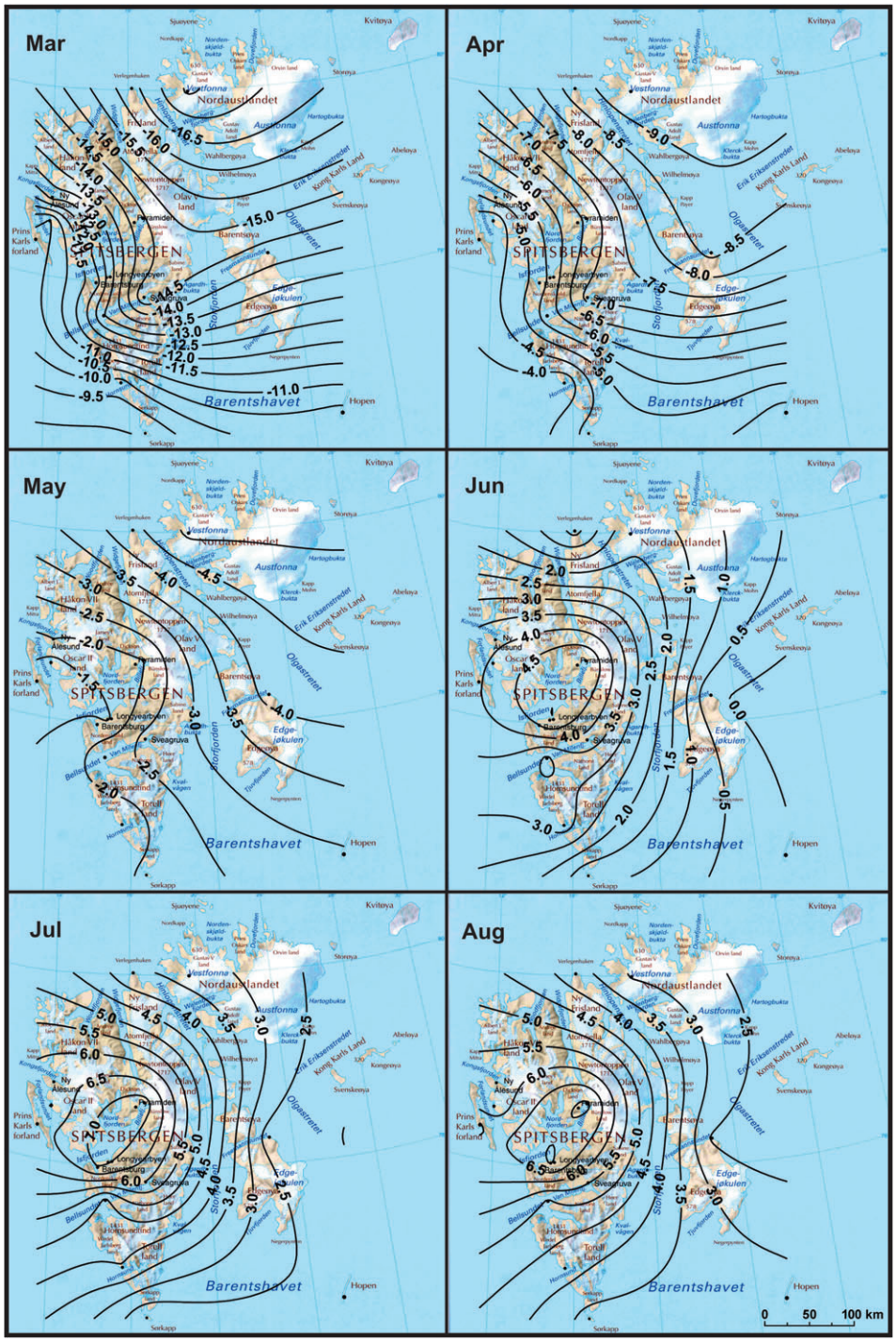

Figure A2. Mean monthly air temperature (°C) at sea level in Svalbard (March 2011 to August 2011).

References

Alissow BP. 1954. *Die Klimate der Erde*. Deutscher Verlag der Wissenschaften: Berlin.

Araźny A. 2008. *Bioclimate of Norwegian Arctic and its Variability in Period 1971–2000*. Wydawnictwo UMK: Toruń (in Polish).

Birkeland BJ. 1920. The climate of Spitsbergen. In *Naturen*, Vol. **44**. Bergen Museum: Norway; 278–288.

Dove HW. 1852. *Die Verbreitung der Wärme auf der Oberfläche der Erde: erläutert durch Isothermen. thermische Isanomalen und Temperaturcurven*. D. Reimer: Berlin.

Dybwad J. 1913. *Observations Meteorologiques faites au spitsberg par l'expedition Isachsen 1909–1910. et systematisees par Aage Graarud*. Kristiania en Commission Chez, Kristiania.

Ewert A. 1972. About calculating thermic continentality of climate. *Prz. Geogr.* **44**: 273–328(in Polish).

Ewert A. 1997. Thermic continentality of the climate of the polar regions. *Probl. Klim. Pol.* **7**: 55–64(in Polish).

Førland EJ, Benestad RE, Flatøy F, Hanssen-Bauer I, Haugen JE, Isaksen K, Sorteberg A, Ådlandsvik B. 2009. Climate development in Noth Norway and the Svalbard region during 1900–2100. *Raportserie.* **128**, 43pp.

Førland EJ, Hanssen-Bauer I, Nordli PØ. 1997. Climate statistic and longterm series of temperature and precipitation at Svalbard and Jan Mayen. DNMI Report. 21/97. Klima. Norwegian Meteorological Institute: Oslo, pp. 43.

Gavrilova LA, Sokolov SI. 1969. Temporal variability of air temperature in the Arctic. In *Trudy Arkt. i Antarkt. Nauchno-Issledov. Inst*, Vol. **287**. Gidrometeoizdat: Leningrad (in Russian).

Haakenstad H, Reistad M, Haugen JE, Breivik Ø. 2012. Update of the NORA10 hindcast archive for 2011 and a study of polar low cases with the WRF model. met.no report 17/2012. Norwegian Meteorological Institute: Oslo.

Hagen JO, Liestøl O, Roland E, Jørgensen T. 1993. Glacier Atlas of Svalbard and Jan Mayen. *Norsk Polarinst. Medd.* **129**: 141.

Hann J. 1887. Atlas der meteorology. In *Berghaus' Physikalischer Atlas*. Justus Perthes: Gotha; 3.

Hanssen-Bauer I, Solas MK, Steffensen EL. 1990. The climate of Spitsbergen. DNMI Rapport 39/90. Klima. Norwegian Meteorological Institute: Oslo.

Hisdal V. 1985. *Geography of Svalbard*. Norsk Polarinstitutt: Oslo.

Hoel A. 1929. The Norwegian Svalbard Expeditions 1906–1926 – Resultater av de Norske statsunderstøttede Spitsbergenekspedisjoner. In *Skrifter om Svalbard og Ishavet*, Vol. **1**. Jacob Dybwad: Oslo.

Hogewind W, Bissolli P. 2011. Operational maps of monthly mean temperature for WMO Region VI (Europe and Middle East). *I* dőjárás. *Quart. J. Hung. Met. Serv.* **115**: 31–49.

Isaaks EH, Srivastava RM. 1989. *An Introduction to Applied Geostatistics*. Oxford University Press: New York, NY; 561.

Ivanov NN. 1959. Belts of continentality on the globe. *Izvest. Wsesoj. Geogr. Obschest.* **91**: 410–423(in Russian).

Käsmacher O, Schneider C. 2011. An objective circulation pattern classification for the region of Svalbard. *Geogr. Ann.: Ser. A, Phys. Geogr.* **93**: 259–271, DOI: 10.1111/j.1468-0459.2011.00431.x.

Kejna M. 2012. Primary climatic controls. In *Topoclimatic Diverisity in Forlandsundet Region (NW Spitsbergen) in Global Warming Conditions*, Przybylak R, Araźny A, Kejna M (eds). Oficyna Wydaw. "Turpress": Toruń; 17–25.

Kotlyakov VM. 1998. *Resources and Environment. World Atlas*. Institute of Geography. Russian Academy of Sciences: Moscow.

Láska K, Witoszová D, Prošek P. 2012. Weather patterns of the coastal zone of Petuniabukta, central Spitsbergen in the period 2008–2010. *Pol. Polar Res.* **33**: 297–318.

Marsz A. 1995. *Index of Thermic Oceanity as Measure of Climatic Works in Ocean–Atmosphere-Continents System*. WSM. WN: Gdynia (in Polish).

Nathorst AG. 1909. *Swedish explorations in Spitzbergen 1758–1908*, Vol. **1**. Ymer: Stockholm.

Nordli Ø. 2010. The Svalbard airport temperature series. *Bull. Geogr. Phys. Geogr. Ser.* **3**: 5–26.

Nordli Ø. Przybylak R. Ogilvie AEJ Isaksen K. 2014. Long-term temperature trends and variability on Spitsbergen: the extended Svalbard airport temperature series 1898–2012. *Polar Research*. **33**: 21349. DOI: 10.3402/polar.v33.21349.

Ohmura A. 1984. On the cause of "Fram" type seasonal change in diurnal amplitude of air temperature in polar regions. *J. Clim. Appl. Meteorol.* **4**: 325–338.

Okołowicz W. 1976. *General Climatology*. PWN: Warszawa.

Przybylak R. 1992. The thermic and humidity relations against a background of the circulations conditions in Hornsund (Spitsbergen) in the period 1978–1983. *Dok. Geogr.* **2**: 5–155 (in Polish).

Przybylak R. 2000. Diurnal temperature range in the Arctic and its relation to hemispheric and Arctic circulation patterns. *Int. J. Climatol.* **20**: 231–253.

Przybylak R. 2002. Variability of air temperature and atmospheric precipitation in the Arctic. In *Atmospheric and Oceanographic Sciences Library*, Vol. **25**. Kluwer Academic Publishers: Dordrecht, Netherland; Boston, MA; London.

Przybylak R. 2003. The climate of the Arctic. In *Atmospheric and Oceanographic Sciences Library*, Vol. **26**. Kluwer Academic Publishers: Dordrecht, Netherland; Boston, MA; London.

Przybylak R. 2007. Recent air-temperature changes in the Arctic. *Ann. Glaciol.* **46**: 316–324.

Przybylak R, Maszewski R. 2012a. Atmospheric circulation and dynamic conditions. In *Topoclimatic Diverisity in Forlandsundet Region (NW Spitsbergen) in Global Warming Conditions*, Przybylak R, Araźny A, Kejna M (eds). Oficyna Wydaw. "Turpress": Toruń; 27–51.

Przybylak R, Maszewski R. 2012b. The influence of atmospheric circulation on temperature and humidity conditions. In *Topoclimatic Diverisity in Forlandsundet Region (NW Spitsbergen) in Global Warming Conditions*, Przybylak R, Araźny A, Kejna M (eds). Oficyna Wydaw. "Turpress": Toruń; 139–145.

Przybylak R, Araźny A, Kejna M. 2012. *Topoclimatic Diverisity in Forlandsundet Region (NW Spitsbergen) in Global Warming Conditions*. Oficyna Wydaw. "Turpress": Toruń.

Putnins P, Schallert W, Choate MM, Langdon LC, Bender Jr TA, Stepanova NA, Wallace Jr JA, Tost BJ. 1959. Some meteorological and climatological problems of the Greenland area. Final Rep. June 20. 1958- July 31. 1959. Sponsored by U.S. Army Signal Research and Development Laboratory. Fort Monmouth: New Jersey, NJ; Weather Bureau: Washington D.C.

Reistad M, Breivik Ø, Haakenstad H, Aarnes OJ, Furevik BR, Bidlot J. 2011. A high-resolution hindcast of wind and waves for the North Sea. the Norwegian Sea. and the Barents Sea. *J. Geophys. Res.* **116**: C05019, DOI: 10.1029/2010JC006402.

Sochrina RF, Tchelpanova OM, Sharova VJ. 1959. *Atmospheric pressure, air temperature and atmospheric precipitation of the Northern Hemisphere: Atlas of maps*. Gidrometeorologitcheskiye Izdatelstvo: Leningrad (in Russian).

Steffensen E. 1969. The climate and its recent variations at the Norwegian Arctic stations. In *Meteorol. Ann.*, **5**(8): 217–349.

Steffensen E. 1982. The climate at Norwegian Arctic stations. Klima DNMI Report. 5. Norwegian Meteorological Institute: Oslo.

Steffensen E. Nordli Ø. Hanssen-Bauer I. 1996. Station history of Norwegian measurements in the Arctic. DNMI-rapport. 17/96. Norwegian Meteorological Institute: Klima, Norway.

Stroeve JC, Serreze MC, Holland MM, Kay JE, Maslanik J, Barrett AP. 2012. The Arctic's rapidly shrinking sea ice cover: a research synthesis. *Clim. Change* **10**: 1005–1027, DOI: 10.1007/s10584-011-0101-1.

Szupryczyński J. 2007. Exploration of Spitsbergen. *Prz. Geogr.* **79**(3–4): 567–592 (in Polish).

Treshnikov AF. 1985. *Atlas of the Arctic*. Glavnoye Upravlenye Geodeziy i Kartografiy pri Sovete Ministrov: Moscow (in Russian).

Undén P. Rontu L. Järvinen H. Lynch P. Calvo J. Cats G. Cuaxart J. Eerola K. Fortelius C. Garcia-Moya JA. Jones C. Lenderlink G. McDonald A. McGrath R. Navascues B. Nielsen NW. Ødegaard V. Rodriguez E. Rummukainen M. Rööm R. Sattler K. Sass BH. Savijärvi H. Schreur BW. Sigg R. The H. and Tijm A. 2002. HIRLAM-5 Scientific Documentation. HIRLAM-5 Project. Available from SMHI. S-601767 Norrköping. Sweden.

Uppala SM, Kållberg PW, Simmons AJ, Andrae U, da Costa Bechtold V, Fiorino M, Gibson JK, Haseler J, Hernandez A, Kelly GA, Li X, Onogi K, Saarinen S, Sokka N, Allan RP, Andersson E, Arpe K, Balmaseda MA, Beljaars ACM, van de Berg L, Bidlot J, Bormann N, Caires S, Chevallier F, Dethof A, Dragosavac M, Fisher M, Fuentes M, Hagemann S, Hólm E, Hoskins BJ, Isaksen L, Janssen PAEM, Jenne R, McNally AP, Mahfouf JF, Morcrette JJ, Rayner NA, Saunders RW, Simon P, Sterl A, Trenberth KE, Untch A, Vasiljevic D, Viterbo P, Woollen J. 2005. The ERA-40 reanalysis. *Quart. J. R. Meteorol. Soc* **131**: 2961–3012, DOI: 10.1256/qj.04.176.

Ustrnul Z, Czekierda D. 2003. Construction of the air temperature maps for Poland using GIS. *Arch. Fotogr. Kart. i Teledet.* **13A**: 243–254 (in Polish).

Walczowski W, Piechura J. 2011. Influence of the West Spitsbergen Current on the local climate. *Int. J. Climatol.* **31**: 1088–1093, DOI: 10.1002/joc.2338.

